Chaos, Solitons and Fractals 38 (2008) 1457–1467

Contents lists available at ScienceDirect

Chaos, Solitons and Fractals

journal homepage: www.elsevier.com/locate/chaos

# Optimization of Euclidean distance threshold in the application of recurrence quantification analysis to heart rate variability studies

Hang Ding *, Stuart Crozier, Stephen Wilson

*School of Information Technology and Electrical Engineering, University of Queensland, Brisbane, 4072 Queensland, Australia*

ARTICLE INFO

*Article history:*
Accepted 16 July 2006

ABSTRACT

An integrated approach is proposed to solve the optimization problem of the Euclidean distance threshold $\varepsilon$ in recurrence quantification analysis (RQA), which is increasingly applied in the study of heart rate variability (HRV). In this paper, $\varepsilon$ is inversely computed from a given recurrence rate (REC), the percentage of recurrence points. From the inversely computed $\varepsilon$, two other RQA output variables: determinism (DET), the percentage of recurrence points forming diagonal line structures, and laminarity (LAM), the percentage of recurrence points forming vertical and horizontal structures, are computed out as well. The trend of DET, LAM values at different REC levels (DLR trend) is introduced to comprehensively represent the dynamic properties of a time series. Based on the DLR trend, the variation of discrimination power, represented by the average loss (or Bayes risk), of DET and LAM, at different REC values is analyzed. Surrogate techniques are used to generate reliable test data sets for the discrimination evaluation. In particular, the results show that (1) the optimal REC can be much higher than the widely used 1% REC, and (2) after the optimization, the average loss can be reduced compared to 1% REC. It is also demonstrated that the optimal $\varepsilon$ depends on the dynamic source and RQA variables, and the DLR trend based $\varepsilon$ optimization method can improve RQA discrimination analysis especially for the short term HRV analysis.



## 1. Introduction

The use of recurrence quantification analysis (RQA) for the nonlinear analysis of heart rate variability (HRV) is of increasing utility [6–10]. RQA is based on the recurrence plot (RP), which permits visualization of hidden recurring patterns [1–4]. The RQA output variables quantify the RP structures and provide some insight into a deterministic chaotic system [2–5]. It has been suggested that the heart rate control system is a nonlinear, chaotic system modulated primarily by the autonomic nervous system [7]. Recurrences within a state space, one of the typical properties of a deterministic chaotic system, are found in the series of consecutive RR intervals, the intervals between the R waves of the electrocardiogram, which mark the onset of the ventricular activation [7,11–15]. Recent studies have demonstrated that RQA output variables can effectively characterize the HR dynamic behavior [1,2,8,10]. Compared with many classical nonlinear analysis methods, RQA has the distinct advantage of not requiring long experimental data series to capture chaotic properties and is relatively immune to noise and nonstationarity.

RQA is very sensitive in detecting any dynamic change; however, it can be easily influenced by the value of the setup parameters. One critical setup parameter for RQA analysis is the Euclidean distance threshold $\varepsilon$. A small variation of $\varepsilon$ can dramatically affect the RQA measures. On one hand, the RP requires a minimal percentage of recurrences to represent original information [16], too small value of $\varepsilon$ may result in quantification of much noise and a very low recurrence rate (REC),

* Corresponding author.
*E-mail address:* hdingmailbox@yahoo.com (H. Ding).

0960-0779/$ - see front matter Crown Copyright © 2008 Published by Elsevier Ltd. All rights reserved.
doi:10.1016/j.chaos.2006.07.059

the percentage of recurrence points, [9,17]; while, on the other hand, too large values of $\varepsilon$ may produce false recurrences or saturate the measurement [3,6]. Eckmann [1] chose $\varepsilon$ by finding a minimal number of neighbors as the setup criterion. Zbilut, under consideration of quantifying the "true" recurrences, suggested setting a small value of $\varepsilon$ where approximately 1% recurrence rate (REC), is reached [6]. Marwan experimentally set $\varepsilon = 0.1 \cdot \sigma$ ($\sigma$: standard deviation) [10]. The $\varepsilon$ setup normally results in relatively higher REC values, and will be influenced by dynamic distributions, which in many cases are not Gaussian. Censi et al. [18] sets $\varepsilon$ at 15% of the maximum distance, which can be subject to spike noise. In addition, recurrence structure in the RP is not a unique property for chaotic systems, as white noise can also produce recurrences [17]. The above methods all use different criteria to choose $\varepsilon$. When applying RQA to very short term HRV analysis, which may allow the real time prediction of cardiac events, the $\varepsilon$ setup becomes more uncertain, as the RQA output variables in a short segment may disperse significantly due to the dynamic noise, fractal dimension, and nonstationarity.

The objectives of this study are to find a practical approach to evaluate the discrimination power of RQA variables and to determine the optimal $\varepsilon$ value, especially for RQA application to short segment HRV analysis. Since there are different criteria to select $\varepsilon$, the $\varepsilon$ value here is inversely computed from a given REC by using its monotonic relationship to REC. From the inversely computed $\varepsilon$, two other RQA output variables: determinism (DET), the percentage of recurrence points forming the diagonal line structures, and laminarity (LAM), the percentage of recurrence points forming vertical and horizontal structures, are computed out as well. The trend of DET, LAM measures at different REC levels (DLR trend) is introduced to comprehensively represent the dynamic properties. In practice, the three RQA output variables: DET, LAM and REC are, respectively, designated as *X*, *Y* and *Z* Cartesian coordinates; A DLR trend is obtained by plotting a series of DET, LAM and REC values in the DLR space, while REC discretely increases from 0% to 100%. Based on the DLR trend, we frame the problem of choosing $\varepsilon$ as a problem of optimizing the discrimination power of DET and LAM over the different REC values. The discrimination power of the DET, and LAM at different REC values is evaluated by the average loss function, which is based on Bayesian statistics, and numerically estimated by a Parzen-type estimator with a Gaussian kernel. To assess the DLR trend visualization and optimization, the surrogate techniques are applied to the time series from Henon, Lorenz, and real heart rate dynamics to generate reliable test data set.

The outline of the paper is the following. In Section 2, the main RQA techniques, surrogate techniques, the Average Loss (Bayes risk), and probability density function (PDF) estimations are briefly reviewed. Additionally, the DLR trend and its evaluation method are introduced. Section 3 demonstrates some typical dynamic systems in the DLR trend, and analyzes the variation of discrimination power of DET and LAM at different REC values. Section 4 presents the findings that relatively high REC values are beneficial for better discrimination power. In the final Section 5, we summarize the findings and potential applications in the future.

## 2. Methods

### 2.1. Recurrence plot, RQA, RP setup

The recurrence plot is based on the analysis of the trajectories under an appropriate reconstruction of the dynamics by the time delay-embedding method [1–4]. If the experimental data series are $\{d(1), d(2), d(3), d(4), \ldots, d(M)\}$, the RP can be expressed as

$$R(i,j) = \Theta(\varepsilon - \|Y(i) - Y(j)\|), \tag{1}$$

where $\varepsilon$ is the threshold; $Y$ is the phase space vector. The two components in the delay-embedding construction in phase space are $Y(i)$ and $Y(j)$, which can be mathematically expressed as

$$Y(i) = \{d(i), d(i-\tau), \ldots, d(i-(\mathrm{d}E-1)\cdot\tau)\}, \tag{2}$$

$$\text{and } Y(j) = \{d(j), d(j-\tau), \ldots, d(j-(\mathrm{d}E-1)\cdot\tau)\}, \tag{3}$$

where $i,j = 1,2,3,\ldots,N$. d$E$ is the embedding dimension; and $\tau$ is the time delay; $\varepsilon$ is a predefined threshold; $\|$ represents a normal operator and, in this work, the Euclidean norm is applied. $\Theta$ is the operator of the Heaviside function. The recurrence plot is a $N \times N$ binary array. If the Euclidean distance between $Y(i)$ and $Y(j)$ is less than the threshold $\varepsilon$, $R(i,j)$ is 1; If greater than $\varepsilon$, $R(i,j)$ is 0. The $N \times N$ binary array is finally marked with the white (0) and black (1).

A recurrence point in the RP means that the dynamic difference of two points with a phase shift in the experimental series falls in a relatively low range (defined by the threshold $\varepsilon$) in the phase space. The REC measures the density of the recurrence points by counting the points in the RP, when $\varepsilon$ is given

$$\mathrm{REC} = \frac{1}{N^2}\sum\nolimits_{i,j=1}^{N} R(i,j), \tag{2}$$

where $R(i,j)$, $i$, $j$ and $N$ are the same as those in Eq. (1).

The diagonal lines represent the dynamics repeating themselves in the phase space. It is quantified by the DET, which is the percentage of the recurrent points that form upward diagonal line segments:

$$\mathrm{DET} = \frac{\sum_{S=S_{\min}}^{N} s \cdot P_s(S)}{\sum_{i,j=1}^{N} R(i,j)}, \tag{3}$$

where $P_s(s)$: the histogram of the diagonal line at the length of $s$; $S_{\min}$: the minimum length of the diagonal line counted for the DET value.

The percentage of the recurrent points that form vertical or horizontal line segments is LAM, a measure of relatively "quiet" dynamics (Laminar state) in the experimental series. It is mathematically expressed as

$$\mathrm{LAM} = \frac{\sum_{w=w_{\min}}^{N} w \cdot P_w(w) + \sum_{u=u_{\min}}^{N} u \cdot P_u(u)}{\sum_{i,j=1}^{N} R(i,j)}, \tag{4}$$

where $P_u(u)$: the histogram of the vertical line at the length of $u$; $P_w(w)$: the histogram of the horizontal line at the length of $w$; $W_{\min}$: the minimum length of the horizontal line counted for the DET value; $V_{\min}$: the minimum length of the vertical line counted for the DET value.

In this paper, we set $dE = 2$, $\tau = 1$, $W_{\min} = V_{\min} = S_{\min} = 2$.

According to the definition of the DET and the $\varepsilon$, it can be seen that the REC is a monotonically increasing function of $\varepsilon$. Therefore, by using a bisection method, it is straightforward to calculate $\varepsilon$ for a given REC. In our study, the REC over the range 0–100% is pre-sampled at the increment of 0.5%, and the algorithm controls the error within 0.05%.

### 2.2. Methods of surrogate data and evaluation function

Surrogate data methods can determine whether an observed time series has statistically significant deterministic components [19]. As the DET, LAM and REC can represent nonlinear properties, the shuffling and Fourier based surrogate techniques are employed here to create reliable test data pairs to evaluate the nonlinear discrimination power of the DET, and LAM at different REC values, leading to the discrimination between the original dynamics and surrogate dynamics. The aim is to find an optimal REC where original dynamics and their surrogate dynamics can be best discriminated by the distribution density of DET, LAM or a combination thereof.

The shuffling based surrogates take on the same values as the original data by creating permutations without replacement. In other words, shuffling process statistically maintains standard deviation and mean and destroys any serial correlation among the data. To study the intervening stages between the original data and surrogates, a swapping method is applied, by which two random addresses along the data series are generated, and the data pointed to by the two addresses are swapped. The times of swapping is parameterized here as TOS. The swapping process also destroys any serial correlation, and has the same effect as the shuffling process, when TOS is large.

The Fourier based surrogate process method adds Gaussian uncorrelated random increments in the phase coefficients [19,21], but retains the squared amplitudes of components. First, the data series is transformed into frequency domain by Fourier transformation:

$$Ak \cdot e^{j\omega k} = \frac{1}{\sqrt{N}} \sum_{n=0}^{N-1} (x_n \cdot e^{j2\pi\omega nk/N}), \tag{9}$$

where $A_k$ and $\omega_k$ are the amplitude and phase of the component $k$ in the frequency domain. The surrogate series $\{x_1^s, x_2^s, x_3^s, \ldots x_n^s\}$ is created by multiplying by a random phase $\alpha_k$ and then transforming back to the time domain:

$$x_n^s = \frac{1}{\sqrt{N}} \sum_{k=0}^{N-1} (Ak \cdot e^{j\omega k} \cdot e^{jzk} \cdot e^{-j2\pi\omega nkN}), \tag{10}$$

where $\{\alpha_1, \alpha_2, \alpha_3, \ldots, \alpha_k, \ldots, \alpha_n\}$ are independent uniform random values within a range

$$-\beta \cdot \pi < \alpha_k < \beta \cdot \pi \quad (\beta >= 0). \tag{11}$$

If $\beta$ is zero, the surrogate dynamics will be identical to the original dynamics. The phase noise will increase as $\beta$ increases.

The objective criterion applied to represent the discrimination power is the average loss function, also known as conditional risk function. The diagram shown in Fig. 1 describes the surrogate model applied here.

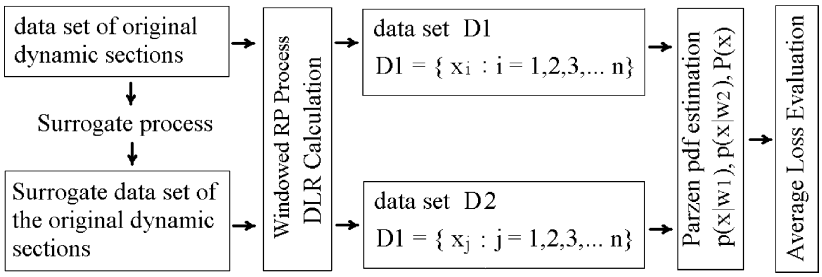


**Fig. 1.** Evaluation process flow chart.

In the discrimination process, the surrogate series are created from the original dynamic series by shuffling and Fourier based surrogate methods. Original dynamic data set of $D1 = \{x_i: i = 1,2,3,\ldots,n\}$ and surrogate data set $D2 = \{x_j: j = 1,2,3,\ldots,n\}$ are generated. The collection of $D1$ and $D1$ forms the unlabeled data set $D = \{x_m: m = 1,2,3,\ldots,n,\ldots,2 \times n\}$. Corresponding to this study, the two classes of original dynamics and surrogate dynamics are denoted as $w1$, and $w2$, and $\Omega = \{w1, w2\}$. The average loss function $\mathscr{L}(D(w_i) \mid \mathrm{REC})$ describes the average loss of decision action, at a given observed REC, and is expressed as [20]

$$L(\mathscr{D}(w_j) \mid \mathrm{REC}) = \sum_{wi} \lambda(\mathscr{D}(w_j), w_i) P(w_i \mid x)|_{\mathrm{REC}}, \tag{5}$$

where $\mathscr{D}(w_i)$ is the optimal decision action:

$$\mathscr{D}(w_j) = \underset{wj \to \Omega}{\operatorname{argmax}} P(w_j \mid x) \tag{6}$$

the loss function $\lambda(\mathscr{D}(w_j), w_i)$ is formulated as

$$\lambda(\mathscr{D}(w_j) \mid w_i = \begin{cases} 0 & \text{if } i = j \\ 1 & \text{if } i \neq j \end{cases} \tag{7}$$

by using the Bayesian rule:

$$P(w_i \mid x) = \frac{p(x \mid w_i) P(w_i)}{p(x)} = \frac{p(x \mid w_i) P(w_i)}{\sum_{w_i \in \Omega} p(x \mid w_i) P(w_i)} \tag{8}$$

The *posterior probability* $P(w_i|x)$ and the *likehood* $p(x|w_i)$ describes the relationship among the classes and the measurements. The *prior probability* $P(w_i)$ is probability of the class $w_i$, and $P(w_1) = P(w_2) = 0.5$, as each original dynamic section results in a corresponding surrogate section in this study. The *evidence* $p(x)$ describes the probability density of unlabeled data set.

### 2.3. Estimation of the probability density function

This study uses the standard Parzen-type method with Gaussian kernels to estimate the probability density function (pdf). An advantage of this method is that it can provide a relatively accurate result even if the experimental data are sparse in some regions. When the number of experimental data points grows and the standard deviation decreases, the estimated conditional probability approaches the true value [22]. The disadvantage is that computation time dramatically increases, when the experimental data series increases in size.

Let $x_1, x_2, x_3, x_4, \ldots, x_n$ be independent random variables identically distributed as a random variable $x$ whose sample distribution function is $f_n$

$$f_n(x) = \frac{1}{n \cdot h} \sum_{j=1}^{n} K\left(\frac{x - x_j}{h}\right), \tag{12}$$

where $h$ is the window width parameter, and $K(y)$ is called a weighting or window function, which must satisfy:

$$-\infty < y < \infty \mid K(y) \mid < \infty, \tag{13}$$

$$\int \mid K(y) \mid \mathrm{d}y < \infty, \tag{14}$$

$$\text{and } \int K(y)\mathrm{d}y = 1. \tag{15}$$

Parzen showed that $f_n(x)$ converges to the true density [22], if

$$\lim_{n \to \infty} h(n) = 0 \text{ and} \tag{16}$$

$$\lim_{n \to \infty} nh^d(n) = \infty. \tag{17}$$

In this paper, we use one of the Parzen weighting functions:

$$K(y) = (2\pi)^{-1/2} \cdot \exp[-y^2/2]. \tag{18}$$

The choice of the window width parameter $h(n)$ is based on the assumption that pdf will be approximately normal with standard deviation estimated by $\sigma_e$, and the optimal value of $h$ is calculated by [23]:

$$h = \sigma_e \left[\frac{8\pi^{1/2} \int K(x)^2 \mathrm{d}x}{3n\{\int x^2 K(x)\mathrm{d}x\}^2}\right]^{1/5}. \tag{19}$$

### 2.4. Dynamic systems and data source

Five dynamic series from Lorenz system, Henon system, Sinusoid wave, white noise and real normal heart rate control system were generated and analyzed to investigate the DLR trend and the discrimination evaluation within the DLR space.

(1) The Lorenz system represents the convective dynamics of fluid warmed from below and cooled from above. All of its state variables are derived from nature, and it exhibits a typical chaotic behavior. The Lorenz series was created where the segments are generated from the standard three coupled ordinary differential equation [24]:

$$\begin{aligned} dx/dt &= -\sigma(x+y), \\ dy/dt &= (\tau - z)x - y, \\ dz/dt &= xy - \beta z, \end{aligned} \tag{20}$$

where the three parameters $\sigma$, $\tau$, $\beta$ are positive and referred to as the Prandtl number, the Rayleigh number, and a physical proportion, respectively. In this paper, standard initiations are applied: $r = 28$; $b = 8/3$; $\sigma = 10$; Initialization is: $x_0 = y_0 = z_0 = 1$. Discrete step size is 0.0002 and the cycle is 1000.

(2) Henon's Poincare plot is a simple one-dimensional curve, but the attractor shows fractal structures. In the RP, it exhibits the typical high and uniform recurrence property. The Henon series is created by the following equation [2]:

$$\begin{aligned} x_n &= 1.0 + y_n - a \cdot x_n^2, \\ y_{n+1} &= b \cdot x_n. \end{aligned} \tag{21}$$

The initialization values are $a = 1.4$, $b = 0.3$, and $y_0 = x_0 = 0.0$.

(3) A sinusoid wave can be seen as a typical linear dynamic, exhibiting a single peak in the frequency domain. The sinusoid wave series for the evaluation is generated by following equation:

$$y_n = 20 \cdot \sin(n \cdot 50/100) \quad (n = 1, 2, 3, \ldots, n, \ldots). \tag{22}$$

(4) White noise follows a Gaussian distribution, and exhibits a broad band in the frequency domain. The white noise series is generated by a random function, and is expressed as

$$x_n = \text{Random}(n) \quad n = 1, 2, 3, \ldots, n, \ldots \quad 0 < \text{Random}(n) < 20.00.$$

(5) Heart rate dynamics are complex and can be seen as a combination of dynamics with white noise. The real heart rate dynamics from the normal sinus rhythm subject (16256) and from the congestive heart failure subject (202) are sourced from PhysioBank [25]. The original atr files are used to generate the heart rate dynamics.

## 3. Result

### 3.1. Characteristic DLR trend properties of different dynamic systems

Different dynamic systems result in different characteristic DLR trends. Fig. 2A shows the five trend groups from Henon, Lorenz, white noise, sine wave, and a subject in normal sinus rhythm. Each group consists of 390 trends computed out from 390 dynamic segments which are randomly extracted from the corresponding dynamic system. The visually separable regions in Fig. 2A shows that each trend group has its characteristic regions. When the averaged trends of each group are plotted in Fig. 2B, the trend characteristics of the five different dynamic systems can be observed more clearly. Generally, the averaged trends of the five dynamic systems originate at the point of (0%,0%,0%), start to diverge at very low REC region (1% > REC), keep diverging in low REC region (1% < REC < 30%), start to converge in middle (30% < REC < 70%) and high (REC > 70%) REC region, and, finally, end at the point of (100%,100%,100%).

By examining the averaged trends projected onto different planes (Fig. 3), it can be seen that: (1) On the DET-REC plane (Fig. 3A), at low REC region, the trends of Lorenz and Henon clearly move toward high DET at low REC range. This property is consistent with high recurrences in chaotic systems. (2) The averaged trends of Lorenz and Henon are very close each other, therefore it may be difficult to use DET to discriminate them. However, in the LAM-REC plane (Fig. 3B), those trends start to diverge at REC values of about 8% (lower dashed line), and diverges up to REC of 30% (upper dashed line), although this divergence does not indicate that the discrimination power is optimal in this range of REC. (3) High DET property does not occur in normal heart rate dynamics (Fig. 3A); In addition the heart rate dynamics has the highest LAM trend among the others (Fig. 3B). (4). As Theil discussed, white noise can also exhibit recurrences [17], although the slope of REC is not as steep as that of a chaotic system (Fig. 3A). (5) The sinusoid exhibits trends similar to those of the other two chaotic systems in Fig. 3A and C, but moves closely with normal heart rate dynamics in Fig. 3B.

Figs. 2 and 3 clearly show that, despite of quantification of false recurrences at high REC region, the DLR trend interestingly exhibits the characteristic correlations among DET, LAM and REC, and the characteristic DLR trend divergences among the five typical dynamic series can be found in a broad REC range. These two facts clearly indicate that the information in relatively high REC regions is valuable, especially, for practical dynamic discrimination analysis.

### 3.2. Surrogate Lorenz and Surrogate heart rate

The great difficulty of the heart rate variability (HRV) study is due to the fact that heart rate dynamics consist of many different dynamic components, including linear, chaotic and stochastic components, and health or disease conditions

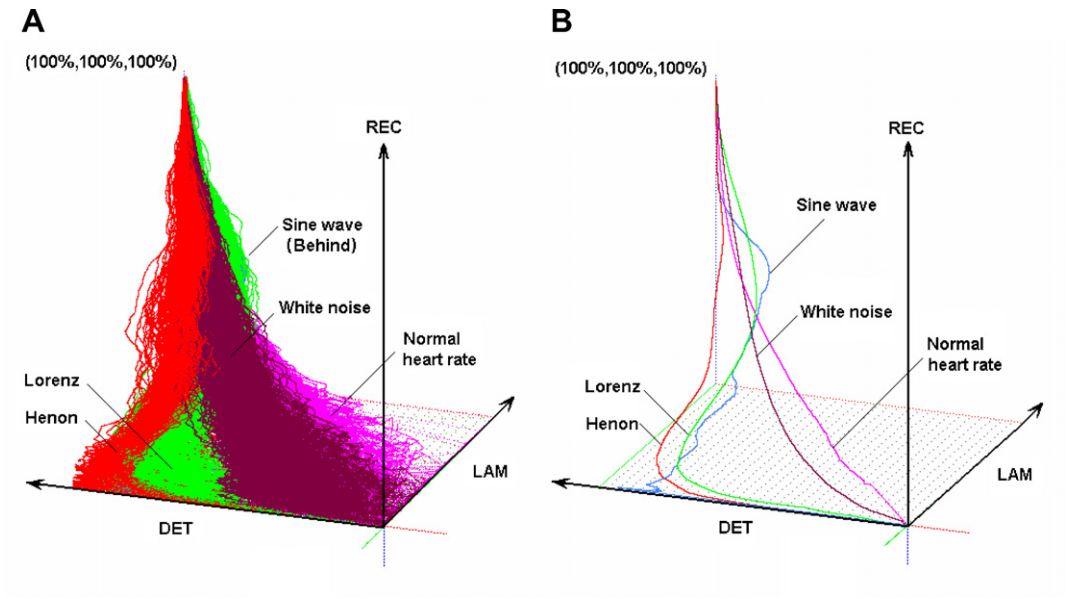


**Fig. 2.** Five DLR trend groups from Henon, Lorenz, Sine wave, normal heart rate and white noise. The characteristic dynamic behaviors of different dynamic systems can be well represented by the DLR trend. (390 segments and RP window size = 120).

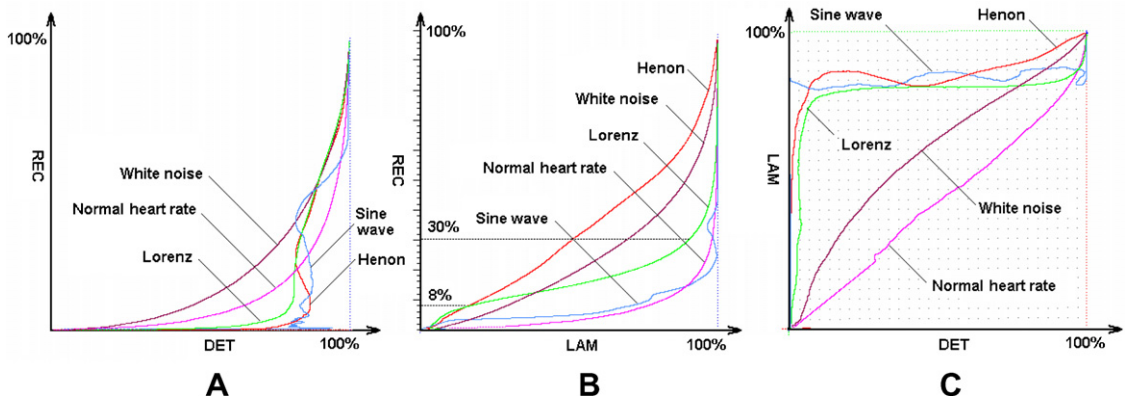


**Fig. 3.** The projection views of the averaged DLR trends from the five groups. Significant DLR trend divergences at relatively high REC regions can be found. A: the projection on DET-REC plan, B: the projection on LAM-REC plane; C: the projection on DET-LAM plane.

valuable for clinical diagnosis may only cause subtle changes in the heart rate control system. In this study, the modified surrogate techniques (described in Section 2) are used to generate some reliable test data set, as the perturbations controlled by TOS or $\beta$ from the two surrogate techniques can be seen as the simulations of two types of subtle control state changes, which, respectively, can not be effectively detected by conventional statistical and spectral HRV analysis methods. As heart rate dynamics tend to be chaotic, a dynamic series from Lorenz is also studied for comparison.

The surrogate Lorenz study shows that Lorenz dynamics has both significant phase correlation in frequency domain and serial correlation in time domain. In Fig. 4, when the phase correlation in the frequency domain is gradually destroyed by increasing $\beta$ by the Fourier based surrogate method, the trends gradually lose the high DET properties, and move toward the white noise trend (refer to the trends in Figs. 2 and 3). Destruction of serial correlation in the time domain can also cause the Lorenz dynamics to lose its dominant high DET (Fig. 5). Fig. 5 also indicates that the underlying dynamic order in the Lorenz system can very easily suffer from noise. When only four swapping operations are undertaken in Lorenz dynamic segments at a length of 120 points, the trend of both DET and LAM of the Lorenz dynamics clearly diverges from its original trend (refer to Fig. 5A). This significant divergence to small phase disturbance and very few swapping operations can be interpreted that the RP for the Lorenz system is very sensitive and well able to capture dynamic changes.

While the Fourier based phase surrogate technique is applied to the normal heart rate dynamics, the differences of averaged DLR trends under different $\beta$ values shown in Fig. 6 are located in a broad REC region, although the differences are not as

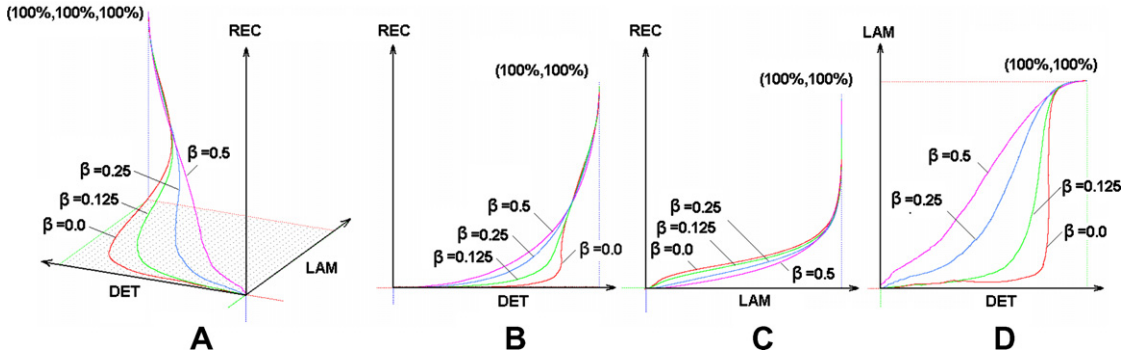


**Fig. 4.** Fourier based surrogate study of Lorenz. While increasing the perturbation in time series correlation, the DLR trend of Lorenz gradually loses its characteristic properties. The significant divergences can be found in the relatively high REC region.

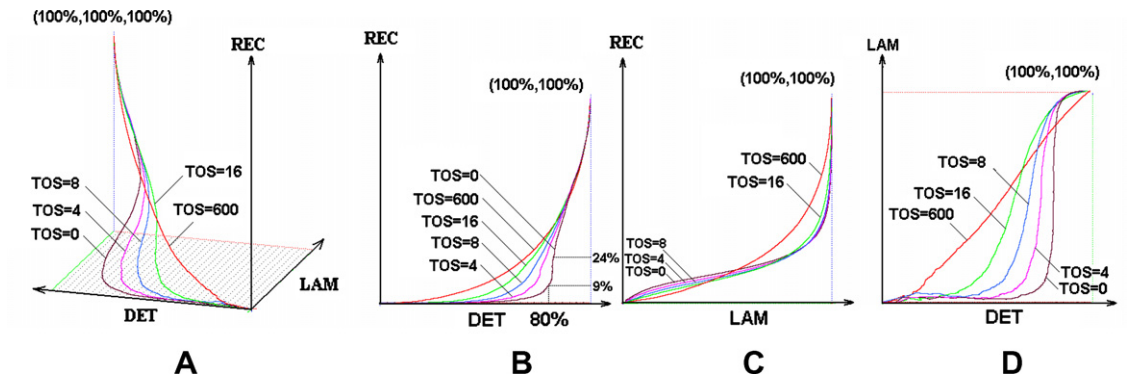


**Fig. 5.** Shuffle based surrogate study of Lorenz. While increasing the perturbation in phase correlation of frequency domain, the DLR trend of Lorenz gradually loses its characteristic properties as well. The significant divergences can be found in the relatively high REC.

significant as those in the Lorenz study. The observable DET variation occupies a wider range of 4.5–58%. The trend variations of LAM are located in the region of 4–37%. The differences of averaged DLR trends from the shuffling based surrogate study significantly show a much broader REC region. On the REC-DET plane (Fig. 7B), the observable divergence occupy in the REC from 3% to 70%. On the REC-LAM plane, the significant differences incur in the 2–69%.

In both surrogate studies, the DLR trend divergences can be observed in broad REC regions, which are much higher than 1% REC. The more significant divergences in relatively high REC region indicate that the DET and LAM measures in those region are more sensitive to detect subtle stochastic perturbations than in very low REC region (REC ⇐ 1%), and, hence, are valuable for discrimination analysis. Additionally, the moderate DET increment in low REC region and insignificant phase

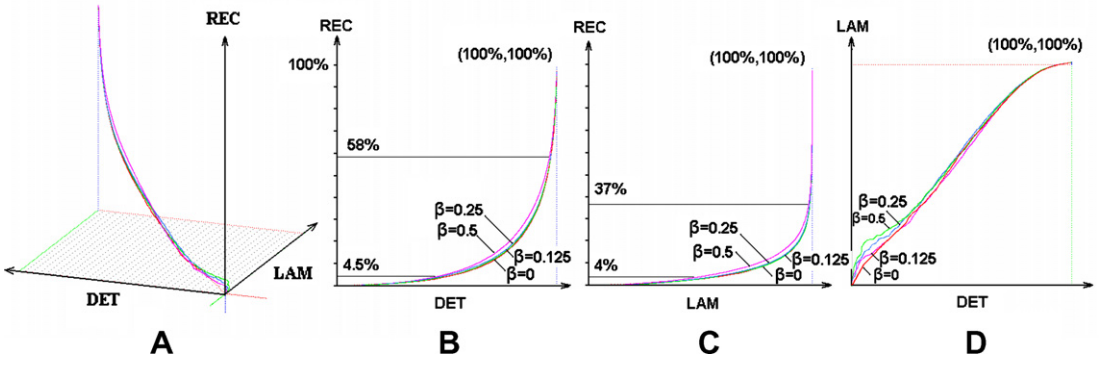


**Fig. 6.** Fourier based surrogate study of normal HR dynamics. The marked levels show the REC region with observable divergences, although the divergences are not significant. Comparing with Fig. 4, the insignificant divergences in surrogate normal heart rate dynamics indicates the heart rate dynamics are different from typical chaotic dynamics, based on which some RQA setups are discussed and suggested.

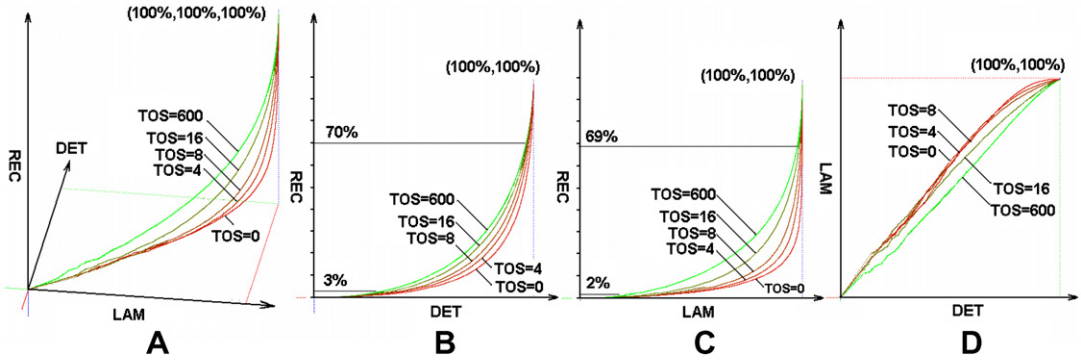


**Fig. 7.** Shuffle based surrogate study of normal HR dynamics. Significant divergences can be found in much high REC regions.

correlation in the normal heart rate dynamics show that the normal heart rate control system is not a typical chaotic system. Therefore, the $\varepsilon$ optimal choice for detecting chaotic systems may not be optimal for the discrimination of heart rate dynamics.

### 3.3. Discrimination power via REC in DLR trends

The more the serial correlations in a Lorenz series are destroyed, the more the Lorenz dynamic properties degrade. How well the DET can discriminate the degrading reflects how well the DET can capture the Lorenz chaotic properties in the first instance. Fig. 8 gives a general view of the variation of the discrimination power of DET at different REC values. It shows 1% REC results in the average loss of 0.071 and the optimal REC locates at 6.5%, where the average loss is less than 0.01. It can also be found that in the band from 4% to 12% the discriminatory power of DET is very low. Examining the trends observed in the DET-REC in Fig. 5B, it is not difficult to see that the Lorenz trend jumps to a high DET level of 80% and keeps relatively constant while the REC varies from about 9% to 24%. Although the divergence of the averaged trends between the trends of the Lorenz and its shuffle based surrogate is larger at 1% REC than at 9.5% REC, the graph of Fig. 9 shows that the probability densities for the Lorenz and its surrogate distribute more widely at 1% REC ("+" marked line in Fig. 9A) than at 9.5% REC ("$x$" marked line in Fig. 9B), and the large overlapping regions in Fig. 9A, which consequently degrades the discrimination power. The average loss of the DET to discriminate Lorenz and Henon in Fig. 8 also interestingly shows that the lowest average loss is at about 10%, rather than 1%.

When analyzing the differences in heart rate dynamics between a normal subject and a CHF subject, RQA parameters, d$E$ = 6 and d$E$ = 10 are also applied, as these two values are suggested by Marwan [5] and Zbilut [7] in their work in this area

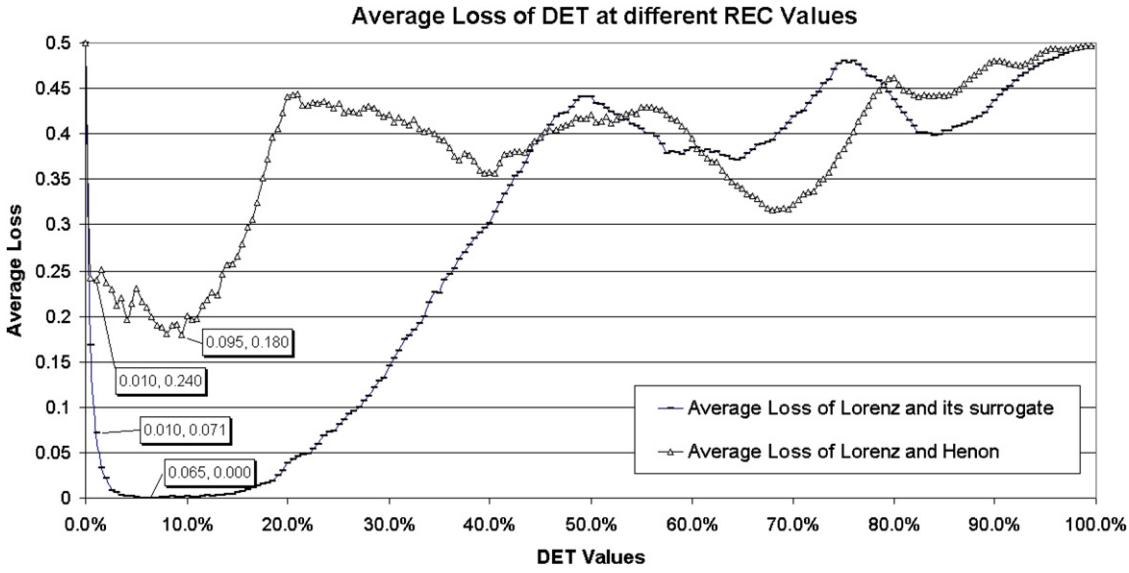


**Fig. 8.** The average loss of Lorenz and its surrogate and the average loss of Lorenz and Henon. The figure shows the significant improvement on discrimination power at the optimal REC sites, compared with the widely used 1% REC setup.

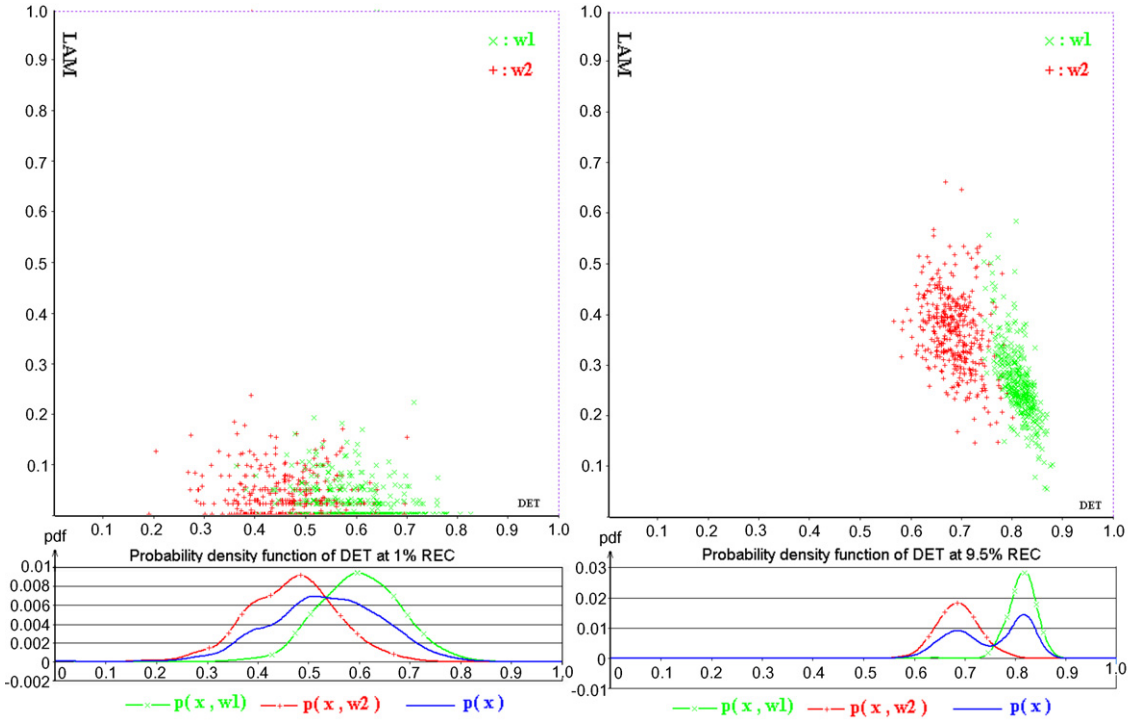


**Fig. 9.** Scatter plots and probability density functions of Lorenz and its surrogate at 1% REC and 10% REC. The 10% REC results in better discrimination power on DET than 1% REC, as the significantly high dispersion at 1% REC degrades the DET discrimination power. ($w1$: Lorenz, $w2$: surrogated Lorenz with TOS = 8, segment length = 120).

of heart rate dynamic analysis. The results, in this case, show that the discrimination power of DET is gradually improved when the REC varies from 0 to 0.50 (Fig. 10). At 1% REC the embedding dimensions of 2, 6 and10 result in the average losses of 0.430, 0.463 and 0.472, respectively. The optimal average losses for these three embedding dimensions are 0.151, 0.242 and 0.256, respectively. The maximum improvement of Average Loss is 0.279 (0.430@1%REC–0.151@45.5%REC). All the corresponding optimal REC values are higher than 40%. The optimal REC values for LAM for the three embedding dimensions are 15%, 4% and 1.5%, respectively (Fig. 11). Comparing Figs. 10 and 11, it can be found that the optimal REC values for the two RQA output variables are not consistent. For DET, optimal REC can locate at very higher REC region (above 40% REC), while for LAM, the optimal REC values can fall in a band from 1.5% to 15%. Generally the 1% REC value does not result in an optimal discrimination power.

The discrimination evaluation results are consistent with the divergence observation and analysis from the DLR trends. The three different dynamic discrimination evaluations of surrogate chaotic dynamic series, typical chaotic dynamic systems, and two real different heart conditions clearly show that, practically, the REC optimization based on the DLR trend can dramatically improve the RQA discrimination power and, especially for the short term heart rate dynamic discrimination, the optimal REC values can much higher than widely used 1% REC.

## 4. Discussion

The trend derived from REC, DET, and LAM (DLR trend) comprehensively reflects the dynamic behavior derived from RQA. Conventionally RQA analysis mainly focus on the recurrence structures extracted by a small Euclidean threshold, as they represent the correlation dimension [21] or are related with the Lyapunov exponents [6,8]. Recently studies suggest that chaotic attractors contain an infinite number of unstable periodic orbits (UPO) [26], which represents the orders within chaos. The RP structures generated from a corridor threshold represent the trajectory, generated by delay-embedding reconstruction, traveling on or near corresponding UPO and can be used to characterize the nonlinear dynamics. Accordingly, an un-thresholded RP (or universal RP proposed by Webber) contains the entire information of a UPO. A thresholded RP is only a part of the un-thresholded RP, although it dramatically simplifies the analysis of the later. When the Euclidean distance threshold $\varepsilon$ increases, REC value monotonically increases, and the RP structures emerge accordingly. DLR trend characterizes the un-thresholded RP in a whole range from small $\varepsilon$ (0% REC) to large $\varepsilon$ (100% REC). Although large $\varepsilon$ can induce false recurrence, this does not practically influence the discriminatory power because the percentage of false recurrences at a given REC also intricately depends on different dynamic systems and can contribute the dynamic discrimination. As the problem of choice

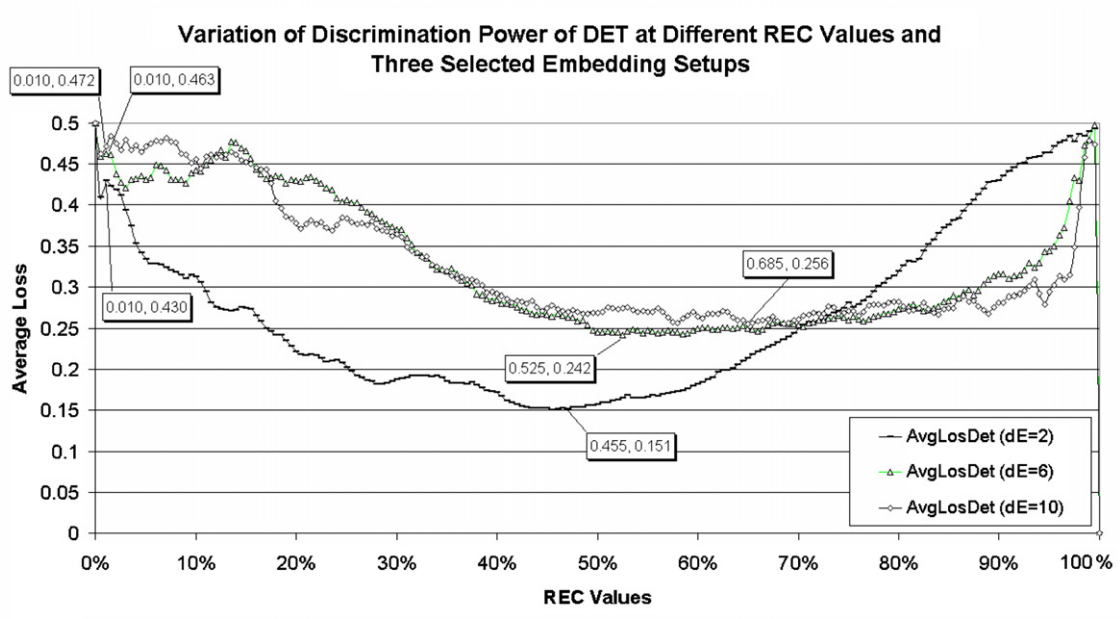


**Fig. 10.** The variation of the average loss of DET at different REC values to discriminate a normal sinus rhythm dynamics and a congestive heart failure dynamics. Three normally used embedding dimensions (2, 6, and 10) for HRV study are applied. Significant improvement on discrimination power of DET can be found at very high REC levels, compared with the 1% REC.

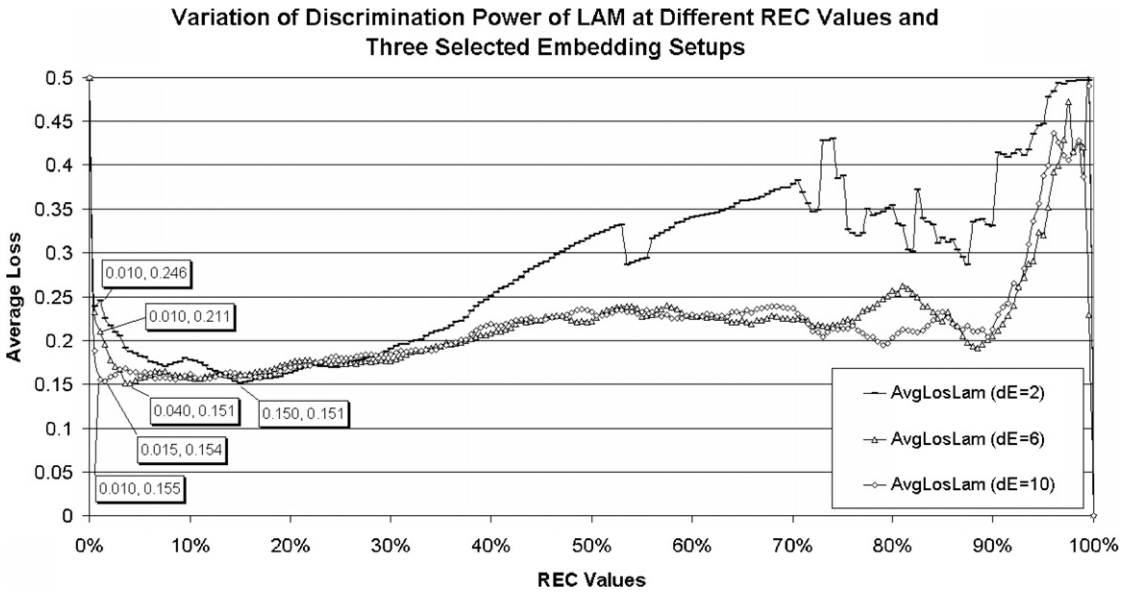


**Fig. 11.** The variation of the average loss of LAM at different REC values to discriminate a normal sinus rhythm dynamics and a congestive heart failure dynamics. Three normally used embedding dimensions (2, 6, and 10) for HRV study are applied. Relatively high REC (10% REC) choices result in better and more reliable discrimination power.

of $\varepsilon$ in the setup vanishes in the DLR trend, the discrimination power evaluation and optimization based on the DLR trend are more reliable and robust. In addition, the DLR trend provides a visual means to observe the dynamic differences in terms of and the trend dispersion and the trend divergence of different dynamic systems.

The large divergence of averaged trends from two dynamic systems at low REC (or small $\varepsilon$) may not result in the optimal discrimination power, because the large divergence distance at lower REC region is also associated with a large dispersion which degrades the discriminatory power. The dispersion is inevitable in the DLR trend as it can be induced by noise, fractal factor, and nonstationarity. When the RP window size is large, and the studied dynamic system has low noise and low fractal

factor and is stationary, this dispersion can be very small. Hence the discriminatory power can be simply determined by the divergence distance. Ziblut's RQA setup strategy of large RP window and low REC value (1% REC) is based on this fact. However, heart rate dynamics are noisy, fractal and non-stationary, and the dispersion becomes dominant especially when a small RP window size, allowing the live prediction of cardiac events, is applied. From the DLR trend in Fig. 2, it can be found that the dispersion increases greatly while REC decreasing. Therefore, the optimal REC shifts from low REC region to relatively high REC region. This point is clearly demonstrated in Fig. 8.

## 5. Conclusion

In summary, the DLR trend method provides a new way to visualize nonlinear dynamic differences. It maintains the nonlinear analysis power of the RQA and extends the DET, and LAM analysis over entire REC range. The most important, the $\varepsilon$ setup vanishes in the DLR trend and hence the RQA discrimination power evaluation is simplified. In the study of discriminating the two simulated chaotic systems and surrogate Lorenz test data set by using DET, the optimal REC value are 9.5% and 6.5%, much higher than widely used 1%. In the study of discriminating a normal heart rate dynamics and congestive heart failure subject, it shows that optimal REC values for LAM are generally higher than 40%, and for DET, the optimal REC value basically fall in a range from 1.5% to 15%. Generally 1% REC does not result in an optimal discrimination power of DET and LAM. After the optimization, the average loss can be reduced by up to 0.279 compared to 1% REC. This study clearly indicates that the optimal REC value depends on the data source and different RQA variables. It can be seen that the RQA discriminatory power can be significantly improved by optimizing the $\varepsilon$ setup and the DLR trend based discriminatory evaluation method allows the $\varepsilon$ optimization in the RQA application of HRV.

## References

[1] Zbilut JP, Santucci Peter A, Yang Shiow Ying, Podolski Janice L. Linear and nonlinear evaluation of ventricular Arrihythmias. In: ISMDA 2002. LNCS, 256. Berlin, Heidelberg: Springer; 2002. p. 151–7.
[2] Guzzetti S, Signorini MG, Cogliati C, Mezzetti S, Porta A, Cerutti S, et al. Nonlinear dynamic and chaotic indices in heart rate variability of normal subjects and heart-transplanted patients. Cardiovascu Res 1996;32(30):441–6.
[3] Zbilut JP, Koebbe Mattew, Use of recurrence plots in the analysis of heart beat intervals. In: IEEE; 1991. p. 263–6 [0276–6574].
[4] Zbilut JP, Tomasson Nitza, Webber Carles L. Recurrence quantification analysis as a tool for nonlinear exploration of nonstationary cardiac signals. Med Eng Phys 2002;24:53–60.
[5] Marwan Norbert. Recurrence qualification analysis to characterize the heart rate variability before the onset of the ventricular Tachycardia. Lect Notes Comput Sci 2001;2199:295–301.
[6] Eckmann JP. Recurrence plot of dynamical systems. Europhys Lett 1987;4(9):973–7.
[7] Webber CL, Zbilut JP. Dynamical assessment of physiological system and states using recurrence plot strategies. Modelling in physiology, The American Physiology Society; 1994 [0161–7567].
[8] Gao Jianbo, Cai Huaqing. On the structures and quantification of recurrence plots. Phys Lett A 2000;270:22.
[9] Casdagli MC. Recurrence plots revisited. Physica D 1997;108:12–44.
[10] Zbilut JP, Giuliani Alessandro. Recurrence qualification analysis and principal components in the detection of short complex signals. Phys Lett A 1998;237:131–5.
[11] Faure Philippe, Korn Henri. A non-random dynamic component in the synaptic noise of a central neuron. Proc Natl Acad Sci Neurobiol 1997;94:6506–11.
[12] Denton TA, Diamond GA. Fascinating rhythm. A primer on chaos theory and its application to cardiology. Am Heart J 1990;120(6 pt 1):1419–40.
[13] Gonzales Juian J, Cordero Juan J. Detection and sources of nonlinearity in the variability of cardiac R–R intervals and blood pressure in rates. Heart Circul Physiol 2000;279(6).
[14] So Paul, Francis JT. Periodic orbits: a new language for neuronal dynamics. Biophys J 1998;74:2776–85.
[15] Mammoliti R, Landini L, Ploa S. Recurrence qualification analysis describes the complex and deterministic behaviour of heart rate variability in healthy subjects. Comput Cardiol 1998;25.
[16] Thiel Marco, Carmen Romano M, Kurths Jurgen. How much information is contained in a recurrence plot. Phys Lett A 2004;330:343–9.
[17] Thiel Marco, Carmen Romano M, Kuths Jurgen, Meucci Riccardo, Allaria Enrico, Tito Arecchi F. Influence of observational noise on the recurrence quantification analysis. Physica D 2002;171:138–52.
[18] Censi F, Barbaro V, Bartolini P, Calcagnini G, Cerutti S. Nonlinear dynamics of atrial rate during atrial fibrillation assessed by recurrence plot analysis. Comput Cardiol 1998;25.
[19] Schreiber Thomas, Schmitz Andreas. Surrogate time series. Chaos 1999;1:27.
[20] Machay David JC. Information theory, inference, and learning algorithms. Cambridge: Cambridge University Press; 2003.
[21] Theiler J, Eubank S, Longtin A, Galdrikian B, Farmer JD. Testing for nonlinearity in time series: the method of surrogate data. Physica D 1992;58:77–94.
[22] Parzen Emanuel. On estimation of probability density function and mode. Ann Math Statist 1962;33:1065–76.
[23] Hand David J. Construction and assessment of classification rules, John Wiley and Sons Ltd. p. 82 [chapter 5].
[24] Abarbanel Henry DJ. Analysis of observed chaotic data. Springer; 1996. p. 29.
[25] Physionet, physiological signal archives for biomedical research. PhysioBank, The Creighton University Ventricular Tachyarrhythmia database. <http://physionet.incor.usp.br/physiobank/database/cudb/>.
[26] Bradley Elizabeth, Mantilla Ricardo. Recurrence plots and unstable periodic orbits. Chaos 2002;V12–3.